Geophysical Prospecting, 1998, **46**, 589–601

Bounds on the complex conductivity of geophysical mixtures[1]

Alan C. Tripp,[2] Elena Cherkaeva[3] and Jeff Hulen[4]

Abstract

Following previous work on bounds for complex dielectrics, bounds on the complex conductivity of a mixture of two isotropic components can be developed which are independent of any special assumption concerning the geometry of the mixture. If certain broad restrictions are assumed, such as isotropy of the mixture, then the bounds can be made more restrictive. These bounds reveal the range of the induced polarization response which can be caused by a mixture of two materials of known complex conductivity. The bounds can also be generalized for spectral responses. The bounds are conservative lithologically in the sense that many of the special models corresponding to boundary responses have lithological counterparts.

The chief use for the given bounds is to gain insight into the nature of the induced polarization response. It is also possible to use the bounds to estimate the volume fractions of the components. We illustrate how this is done for the case of a general anisotropic medium.

Introduction

The ultimate objective of interpreting induced polarization (IP) data is to gain some insight into the composition of a rock. There are two aspects to this task. The first, which we call ‘physical property modelling’, is to deduce a model of the complex resistivity distribution, or an approximation thereof, whose response to impressed sources matches the field data in some optimal sense. The second aspect, which we call ‘lithological modelling’, is to assign a lithological interpretation to each complex resistivity unit. Thus the ultimate goal of an IP survey is to predict the geological distribution of specific minerals of interest, by successful physical property and lithological modelling.

Both modelling methods are dogged by uncertainty. Physical property modelling is a classic example of an ill-posed geophysical problem in that, given typical field data,

---

[1] Received September 1996, revision accepted June 1998.

[2] Department of Geology and Geophysics, 717 Browning Building, University of Utah, Salt Lake City, UT 84112, USA.
[3] Department of Mathematics, University of Utah, Salt Lake City, UT 84112, USA.
[4] EGI, Department of Civil Engineering, University of Utah, Salt Lake City, UT 84112, USA.

there will be a large class of complex resistivity distributions which will model the data equally well. The interpreter must then decide which set of models should be given further consideration or, as is often done, which set of models is closest to preconceptions. The deduced but non-unique physical properties must then be given a geological interpretation. There are large classes of lithologies which have the same macroscopic intrinsic complex resistivities. These uncertainties in the interpretation must be treated using as much valid *a priori* information as possible. Even so, although the IP method is extremely useful in finding ore, the degree of imprecision in giving a geological interpretation to data sets is perhaps underappreciated and is most certainly underquantified.

One procedure employed in induced polarization exploration for disseminated sulphides was the use of various mixing formulae to try to relate the IP measurement to lithology by varying the geometry and concentration of the sulphide (Wait 1982). However, these studies can be viewed in a new light, in so far as composite media theories have given bounds on the effective complex conductivity for very broad assumptions concerning the geometry of the mixture. Moreover, there is a hierarchy of bounds linked by increasingly stringent assumptions, into which previous efforts with spheroids, etc. fall. Furthermore, these bounds can be inverted to volume percentage bounds.

These bounds will be discussed and it will be shown how they might be applied to the lithological interpretation of IP data.

First, we adapt theoretical bounds on complex permittivities of composite materials (Bergman 1978, 1980; Milton 1980, 1981), to give bounds on the complex spectral conductivities of two-component mixtures. These bounds are realized in many situations by specific mixture geometries, which can simulate ore textures.

Secondly, we show how these bounds may be inverted to give bounds on component volume fractions, assuming that the component complex conductivities are known.

Throughout, we have assumed that the complex conductivity distribution of an ore can be approximated using two discrete components. The applicability of this assumption, which is a matter for research, involves petrophysical considerations outside the scope of the paper.

Theory

The strategy followed here is to combine the notion of the mineral complex conductivity spectrum with rigorous and obtainable bounds for composite materials to illustrate the range and character of responses which can be achieved from a two-component mixture. We will briefly present the two ideas and then illustrate how they can be combined.

Mathematical characterization of complex conductivity

The electric constitutive relationship linking a time–harmonic electric current density **J** and the associated time–harmonic electric field **E** is (Harrington 1961)

$$\mathbf{J} = (\sigma + j\omega\varepsilon)\mathbf{E}, \tag{1}$$

where $\sigma + j\omega\varepsilon$ is the admittivity of the medium and is a function of the conductivity σ, the dielectric permittivity ε and the angular frequency ω. Both σ and ε are scalar or tensor complex functions of ω. We assume the convention discussed by Pelton (1977) and relate the entire complex behaviour of the admittivity for typical exploration frequencies below the kHz range to σ.

Because a complex conductivity spectrum can span many frequency decades, representing the response by a few parameters facilitates investigation. A popular method of doing this is to use a superposition of phenomenological Cole–Cole relaxation models of the form

$$\sigma(\omega) = \sigma_0/[1 - m(1 - 1/\{1 + (j\omega\tau)^c\})], \tag{2}$$

where σ_0 is the direct current conductivity, with a subsequent distribution of the parameters c, m and τ (Cole and Cole 1941; Pelton 1977).

We adopt this model and consider only mixtures of two components: one a non-polarizable component and the other a polarizable component represented by a single Cole–Cole dispersion relationship. Generalization of the procedure for components requiring more than one Cole–Cole dispersion is straightforward.

Mathematical bounds on two-component mixtures

Assume that we know the complex conductivities of two components which are mixed together in some fashion. It is possible to find bounds on the bulk complex conductivity of the mixture which are tight in the sense that the bulk conductivity of some mixtures actually lies on the boundary. Moreover, the nature of the bounds gives insight into the uncertainties of lithological interpretation.

The basic theory which we adopt was developed by Bergman (1978, 1980) and Milton (1980, 1981) for bounding the bulk complex permittivity of a mixture of two components of complex permittivities. Because the physically measurable quantities are the electric current **J** and the electric field **E**, bounds on the complex transfer function between them can be referred directly to complex conductivities. For a rigorous derivation and discussion of the basic bounds, see Bergman (1978, 1980) and Milton (1980, 1981).

Assume that a rock is a mixture of materials of two complex scalar conductivities σ_1 and σ_2. These two conductivities, for a specific value of ω, are plotted in Fig. 1, which is broadly based on a figure from Milton (1981). If we assume that nothing is known concerning the geometry or the volume percentage of the component materials, then the diagonal elements of the mixture complex bulk conductivity tensor lie within the region Ω. The upper bound for this region is the straight line connecting σ_1 and σ_2,

$$\sigma = \sigma_1 p_1 + \sigma_2 p_2, \tag{3}$$

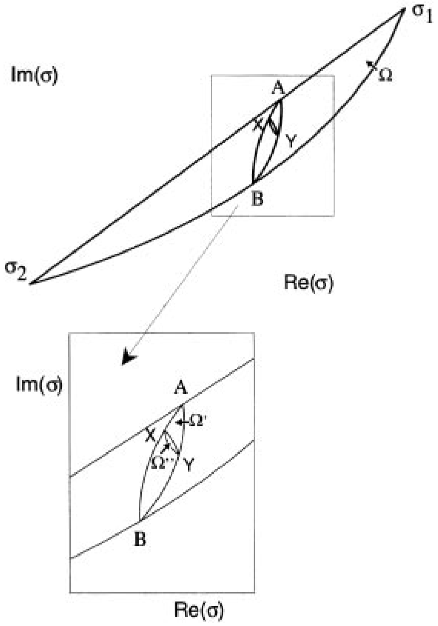

Figure 1. General representation of the bounds in complex conductivity space. The region Ω bounded by the line and the arc passing through σ_1 and σ_2 gives the bounds for the principal values of a general conductivity tensor. The arcs passing through A and B define the region Ω', which bounds the principal conductivities for a particular volume fraction, while the arcs intersecting at X and Y, defining the region Ω'', give the effective conductivity bounds for the particular volume fraction if the material is isotropic.

where p_1 and p_2 are the volume fractions of the components 1 and 2. The lower bound is the arc

$$\sigma = [(p_1/\sigma_1) + (p_2/\sigma_2)]^{-1}. \tag{4}$$

These bounds are actually obtained by the principal values of anisotropic materials consisting of laminations of materials 1 and 2, as shown in Fig. 2. The line boundary gives the bulk conductivity for the principal axis perpendicular to the laminations, while the arc gives the bulk conductivities for the other two principal axes which are parallel to the laminations.

Now assume that we have information concerning the volume fraction of the two components and let the points A and B be the points on the previous line and arc boundaries which correspond to the given volume fraction. Then the area Ω' between the two arcs connecting A and B contains the diagonal elements of the bulk conductivity tensor of all mixtures with the given volume fractions p_1 and p_2. The upper arc is defined by the equation

$$\sigma = \sigma_2 + p_1\sigma_2(\sigma_1 - \sigma_2)/[\sigma_2 + vp_2(\sigma_1 - \sigma_2)], \tag{5}$$

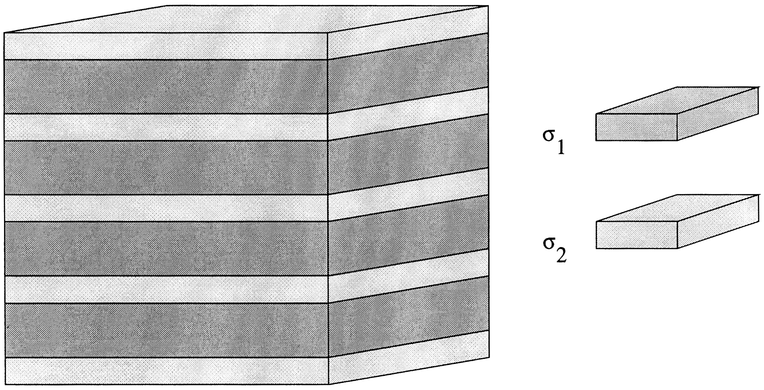

Figure 2. Representation of anisotropic laminated material whose principal conductivities lie on the boundaries of Ω.

where $0 \leq v \leq 1$ parameterizes the curve. The lower arc is defined by the equation

$$\sigma = \sigma_1 + p_2\sigma_1(\sigma_2 - \sigma_1)/[\sigma_1 + vp_1(\sigma_2 - \sigma_1)], \tag{6}$$

where again $0 \leq v \leq 1$. The arc boundaries of Ω' are obtained by the diagonal elements of the conductivity tensor of a coated elliptical cylinder geometry, whose cross-section is shown in Fig. 3. The boundary is also attained by the three principal conductivities of a medium of densely packed coated spheroids. More details concerning the dimensions of the component increments are given by Milton (1981).

If we assume that the material is isotropic, then the bulk conductivity is contained in the region Ω'', bounded by arcs connecting X and Y. These arcs have the form

$$\sigma = p_1\sigma_1 + p_2\sigma_2 - p_1p_2(\sigma_2 - \sigma_1)^2/d[u_1\sigma_1 + u_2\sigma_2], \tag{7}$$

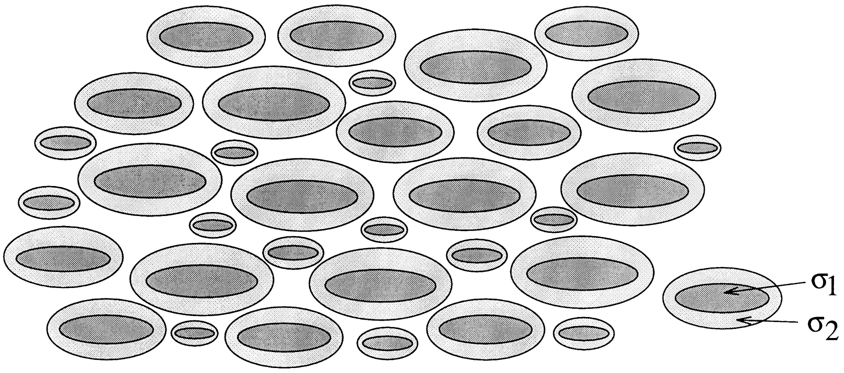

Figure 3. (After Milton 1981). Representation of a coated elliptical cylinder geometry whose principal conductivities attain the boundaries of Ω'. The placement of σ_1 and σ_2 in core and coating, or vice versa, determines the particular arc upon which the principal conductivities will fall.

where $u_1 \geq p_2/d$ and $u_2 \geq p_1/d$ are varied subject to the constraint $u_1 + u_2 = 1$, and

$$\sigma = [p_1/\sigma_1 + p_2/\sigma_2 - (d-1)p_1p_2(1/\sigma_2 - 1/\sigma_1)^2/d[u_1/\sigma_1 + u_2/\sigma_2]^{-1}, \tag{8}$$

where $u_1 \geq p_2(d-1)/d$ and $u_2 \geq p_1(d-1)/d$ are varied subject to the constraint $u_1 + u_2 = 1$. In both of these expressions, d is the dimensionality of the mixture; in our case $d = 3$. These bounds are generalizations into the complex space of the more familiar Hashin–Shtrikman bounds for a real conductivity (Hashin and Shtrikman 1962). The assumption that the composite is isotropic constrains the bounds for the bulk conductivity dramatically, and hence a correct assumption of isotropy is very useful. On the other hand, assuming an anisotropic medium is isotropic can drastically bias the range of possible bulk conductivities and hence in the inverse sense can lead to poor estimates of volume fractions and component identities. For any given frequency, it is always true that $\Omega'' \subset \Omega' \subset \Omega$.

The boundary of Ω'' defined by (7) is attainable at five points by known composites, as discussed by Milton (1981). Hence this boundary is tight in so far as any other bounds must touch these bounds at least at the five attainable points. The boundary described by (8) is actually not attainable by an isotropic material and hence the boundary is too liberal and a tighter bound is conceptually possible.

Spectral bounds

Because the resistivities of rock matrix and semiconducting ore minerals are typically orders of magnitude apart in value, the bounds which we are discussing enclose a very large region of complex conductivity space, even when some stringent geometric restrictions, such as property isotropy, are imposed. Because the bounds are attainable, this state of affairs is not an indictment of the bounds but rather reveals the versatility which nature possesses in achieving a range of complex conductivities with two simple components. Of course, the very range of responses attainable by a two-component mixture makes the lithological interpretation problem very difficult. Thus, given a certain complex conductivity measurement, how can one hope to deduce the identity and geometry of the components given the range of responses possible from a mixture? Although we discuss this problem below, an additional constraint on the problem which can be of use is the variation of the effective conductivities with respect to frequency. That is, the bounded regions of effective conductivity space will vary as a function of frequency if the component conductivities vary as a function of frequency.

To illustrate this effect, first consider Fig. 4. This figure illustrates the complex spectra for two components of a mixture. The first component has a real DC value of σ which we have assumed for simplicity to be 1. Its complex response is governed by a Cole–Cole dispersion with the parameters $c = 0.5$, $m = 0.1$ and $\tau = 0.5$. The response is calculated at one point per decade from $\omega_1 = 0.0001$ rad/s to $\omega_7 = 1000$ rad/s. The second component is assumed to be non-polarizable, with a real part of 0.5. The contrast between the real values of σ_1 and σ_2 has been kept artificially low to facilitate an informative plot.

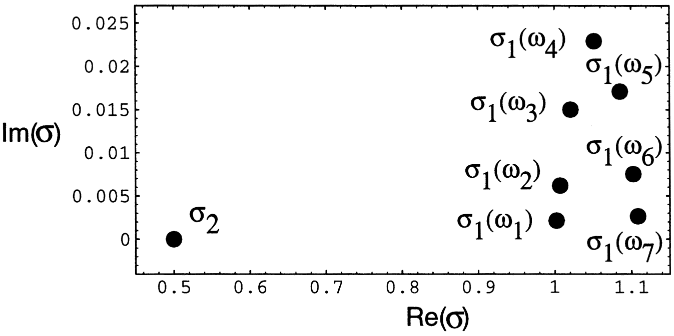

Figure 4. Sample spectral response for a polarizable material, calculated from $\omega_1 = 0.0001$ rad/s to $\omega_7 = 1000$ rad/s at one point per decade.

Figure 5 illustrates the region Ω as a function of the excitation frequency. These dynamic bounds are applicable for any geometric arrangement of the two components. Assumptions concerning component volume fraction or mixture isotropy will lead to dynamic bounds for the Ω' or Ω'' regions.

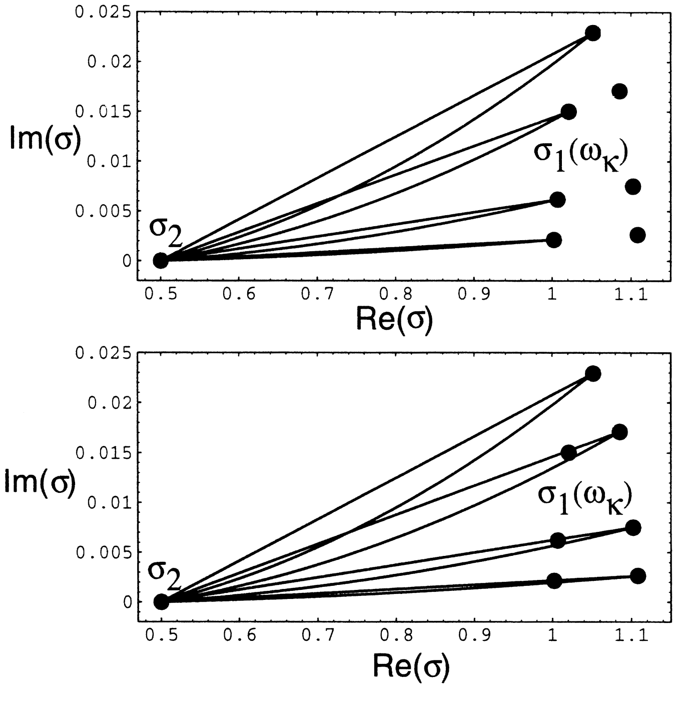

Figure 5. Spectral Ω bounds for the material whose spectral response is illustrated in Fig. 4.

Correspondence of realizable bounds with geological assemblages

The bounds on the effective complex conductivities are in many cases realizable, that is, there are physical mixtures whose conductivities assume boundary conductivities. This is important in so far as the bounds are not too large in the region of these conductivities and the bounds give us an idea of the range of conductivity responses which might in fact be encountered, rather than simply telling us what responses could not be encountered, as do non-realizable bounds. But this does not tell us whether these physically realizable bounds are in fact geologically realizable. This is a difficult question whose explication is beyond the scope of this paper. However, some insight into the problem may be gained if we assume that the geometry of rock texture largely translates into the geometry of electrical conductivity. With this proviso, we now examine the lithological attainability of bounding models with some simple examples of ore textures.

Ore petrology

First consider tabular or elongate-lentoid bodies comprised of alternating highly and poorly conductive planar laminae, which are the natural counterparts of the laminae whose principal conductivities attain the boundaries of Ω.

The best examples of planar-laminated ore textures can be found among deposits formed by subaqueous chemical precipitation and sedimentation directly upon a contemporaneous surface. Those with ore textures best approximating the model include firstly the Precambrian banded iron formations (Garrels, Perry and Mackenzie 1973) and related exhalite gold deposits such as Homestake, USA (Sawkins and Rye 1974), and secondly the ‘black-shale-hosted’ (BSH) deposits such as Sullivan, Canada (Freeze 1966) and Rammelsberg, Germany (Anger *et al.* 1966). The banded iron formations (BIF), which account for most of the world’s iron production, are tabular bodies, up to a square kilometre or more in area and tens of metres thick, consisting predominantly of alternating, millimetre- to centimetre-thick laminae of chert or reddish, haematitic, microcrystalline quartz and magnetite or haematite. The BSH deposits, which can be as large as the BIF, are comprised of comparably sized sulphide laminae, principally galena, sphalerite and chalcopyrite, which may or may not be interstratified with laminae of quartz, sericite, chlorite, barite and the common carbonate minerals in various combinations. Planar-laminated ore textures are also found locally in epithermal precious-metal vein systems such as Oatman, Arizona, although they are not nearly as well developed as in the BIF and BSH deposits. Individual planar laminae in the veins tend to be discontinuous, to ‘pinch and swell’ along strike, and to be disrupted by botryoidal (i.e. appearing like a bunch of grapes) textures. Figure 6 illustrates a ‘geologically laminated’ model.

Geological analogues to the space-filling coated ellipsoidal or spheroidal geometries attaining the boundaries of Ω' are harder to find. Nearly perfect spheroids of any size are extremely rare among metallic mineral deposits, let alone conductive spheroids with

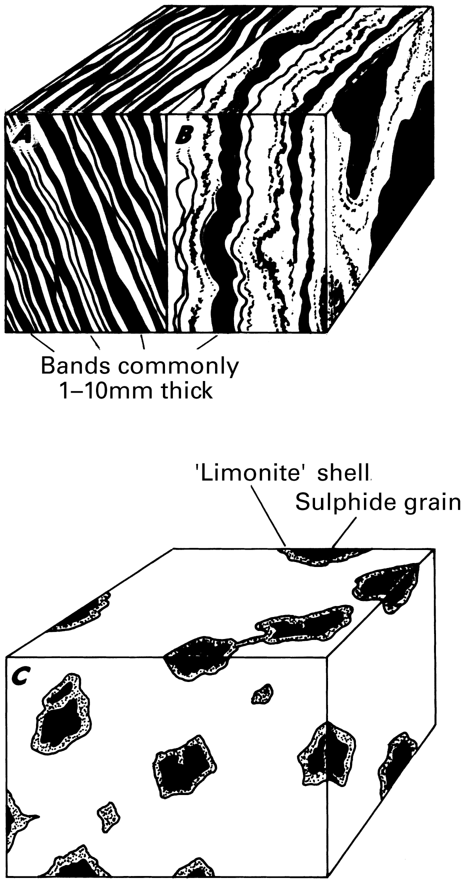

Figure 6. Schematic diagrams of some typical ore textures approximating the complex conductivity models discussed in this paper. **A**: Rhythmically interlaminated textures common in the Precambrian banded iron formations (BIF) and the black-shale-hosted (BSH) sulphide deposits. The black bands represent conductive metallic minerals while the white bands represent poorly conducting phases. **B**: More crudely interlaminated textures commonly found in epithermal precious-metal vein deposits. The black bands, which contain the precious metals, represent electrically conductive metallic sulphides (e.g. chalcopyrite) and sulphosalts (e.g. tetrahedrite). The white bands represent a variety of poorly conductive gangue minerals. **C**: Disseminated textures common in, for example, porphyry copper and Carlin-type gold deposits. In this case, disseminated sulphide, in a poorly conducting matrix, is peripherally oxidized to non-conductive 'limonite'.

non-conductive shells. Perhaps the best natural examples of these spheroids are found in the oolitic iron ores, for example in the Silurian Clinton formation of eastern USA, which are comparable in size to BIF and contain abundant, disseminated, millimetre-sized oolites consisting variably of haematite, goethite, chamosite (iron-rich chlorite) and siderite, commonly embedded in a matrix of clay, calcite or siderite. Many of the oolites consist of alternating shells of these minerals. Those composed entirely of conducting haematite with shells of chamosite, siderite or goethite do occur locally but seldom account for the majority of the oolites in a given orebody.

Imperfect natural analogues for the coated conductive spheroid model can be found among the disseminated sulphide systems typical of, for example, porphyry copper deposits (e.g. Lowell and Guilbert 1970) and Carlin-type sediment-hosted gold deposits (e.g. Percival, Bagby and Radtke 1988). These sulphide systems typically contain 1–10 volume percentage millimetre-sized, roughly equant, although seldom truly spheroidal, hydrothermal sulphide (principally pyrite) grains disseminated throughout matrices of variable composition but commonly containing abundant quartz and sericite or other hydrothermal layer silicates. The closest conceptual match to the model occurs when these sulphides are partially and peripherally oxidized to non-conductive ‘limonite’, dominantly various combinations of goethite and jarosite.

The porphyry copper lithological model has been the subject of a great deal of theoretical and experimental investigation (e.g. Wait 1958; Halverson *et al.* 1981). Figure 6 represents a particular ore lithology.

Component volume fraction estimation

The bounds presented give the global extent of the complex conductivities of a composite material of two components. However, they can also be used to determine bounds for component volume fractions.

Suppose that we have deduced a complex resistivity model and we are confronted with the lithological interpretation problem, i.e. what lithology does a particular complex resistivity unit represent? This problem itself has two components. First, assuming a two-component mixture, what are the conductivities and volume fractions of the components? Secondly, what do these physical properties imply about the lithology? We will illustrate the application of the bounds derived above to one aspect of the first problem by deriving volume fraction bounds for the components of the mixture. This ‘inverse volume fraction’ problem has been considered by McPhedran, McKenzie and Milton (1982) and McPhedran and Milton (1990), who present several numerical inversion schemes. The explicit bounds which we derive below were first presented by Cherkaeva and Tripp (1996).

Suppose that we have a measurement of the effective complex conductivity of a rock unit and that the unit is a mixture of two components. We will assume, as is the case in many exploration scenarios, that one of the components is a background rock which is very poorly polarizable but whose conductivity can be estimated and that some estimate can be made of the complex conductivity of the polarizable component.

Further suppose that we have measured a scalar complex rock conductivity $\sigma(\omega) = (\sigma_r(\omega), \sigma_i(\omega))$ as a function of frequency and we have made some broad assumptions concerning the geometry of the mixture which will determine the bounding region into which the conductivity falls. The lower and upper boundaries of this region for a particular volume fraction p of the polarizable material and a frequency ω are $l(p,\omega)$

and $u(p,\omega)$, respectively. Now since the bounds are all continuous with respect to p, measured $\sigma(\omega)$ will lie on a lower boundary for some p_l and will lie on an upper boundary for some p_u. Hence $\sigma(\omega) = l(p_l,\omega) = u(p_u,\omega)$ and by continuity $p_u(\omega) \le p \le p_l(\omega)$. Now such an expression will hold for every ω and since the ore volume fraction will not change as a function of frequency, a set of bounds will be $\cap_\omega(p_u(\omega), p_l(\omega))$. Hence the inversion algorithm consists of two parts. In the first part, the values $p_u(\omega)$ and $p_l(\omega)$ are determined and in the second part an intersection of the intervals is executed.

If nothing can be said about the geometry of the composite, then the bounded region for the complex conductivities has the form Ω shown in Fig. 1. We will assume that the effective conductivity lies in the interior of this region, since if it lies on one of the boundaries we can uniquely determine the volume fraction of the constituent components.

Hence, for a given frequency, the volume fraction bounds of the polarizable material are

$$p_l = \mathrm{Im}(\tilde{a}_l b_l)/\mathrm{Im}(\mathrm{b}_l) \tag{9}$$

and

$$p_u = 1 - (\mathrm{Im}(\tilde{a}_u b_u)/\mathrm{Im}(b_u)), \tag{10}$$

where $p_l \le p \le p_u$ and $a_u = (\sigma_e - \sigma_1)/(\sigma_2 - \sigma_1)$, $b_u = (\sigma_e - \sigma_1)/\sigma_1$, $a_l = (\sigma_e - \sigma_2)/(\sigma_1 - \sigma_2)$ and $b_l = (\sigma_e - \sigma_2)/\sigma_2$. The value σ_e is identified with the scalar complex conductivity or conductivity principal value of a rock unit, as modelled using field data, and the tilde denotes complex conjugation.

To appreciate the extent of these bounds, consider Figs 7 and 8. Figure 7 gives the Ω bounds for the fourth, or most polarizable, spectral measurement of our sample case, together with an arc which is entirely contained in Ω. This arc is parameterized by a normalized arc-length parameter t, which runs from 0 to 1. Thus any measured

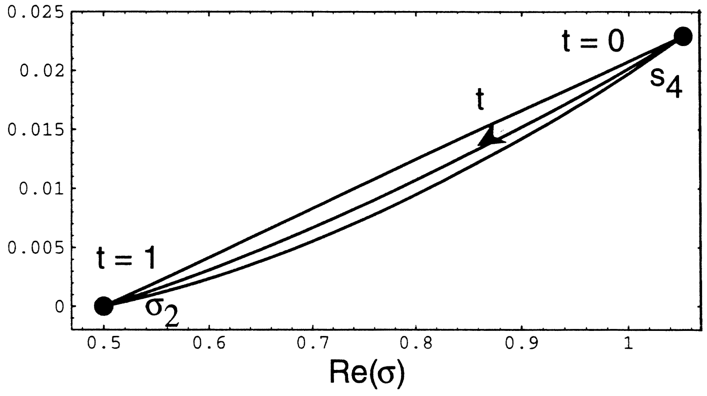

Figure 7. Spectral Ω bound for the fourth spectral measurement together with a curve, parameterized by t, entirely contained in Ω.

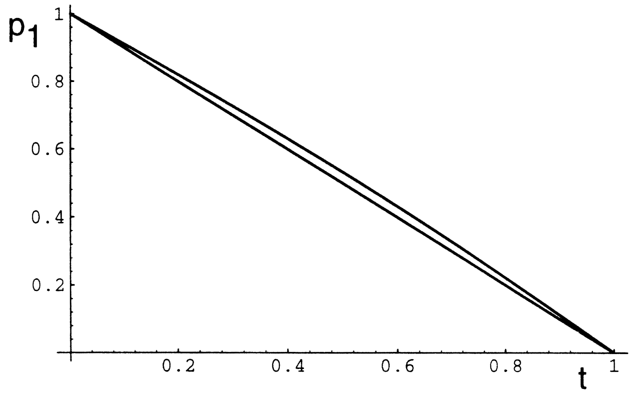

Figure 8. Volume fraction Ω bounds for p_1 as a function of t.

conductivity along the arc can be identified with a value of t and will have associated volume fraction bounds, as given by (9) and (10).

Figure 8 gives a plot of the upper and lower bounds for the volume percentage p_1 of the component 1, plotted as a function of the position of the composite conductivity along the arc, again parameterized in terms of t. The bounds are very small, given the fact that the geometry of the mixture is indeterminate.

If bounds are derived for each spectral measurement, the intersection of all the individual bounds will give global bounds which are never bigger than the smallest of the individual bounds and which could be significantly smaller.

If the mixture is isotropic, bounds for the volume fraction should be derivable in a similar fashion using (7) and (8).

Conclusions

We have discussed the extension of bounds on the bulk dielectric of a two-component mixture to complex conductivity mixtures encountered in the induced polarization technique. These bounds give insight into the range of possible responses arising from two known components, and in particular illustrate what a strong assumption isotropy is in bounding the response. These bounds have been inverted to give bounds on the volume fractions of mixture components, and thus give a formal solution to one aspect of the lithological interpretation problem. Throughout it has been assumed that a particular material could be approximated by a two-component material, which may be difficult in practice.

Acknowledgements

This work was supported by the Department of Energy under grant no. DE-FG03-93ER14313.

References

Anger G., Nielsen H., Puchelt H. and Ricke W. 1966. Sulfur isotopes in the Rammelsberg ore deposit, Germany. *Economic Geology* **61**, 511–536.

Bergman D.J. 1978. The dielectric constant of a composite material – A problem in classical physics. *Physics Reports* **43**, 378–407.

Bergman D.J. 1980. Exactly solvable microscopic geometries and rigorous bounds for the complex dielectric constant of a two-component composite material. *Physics Review Letters* **44**, 1285–1287.

Cherkaeva E. and Tripp A.C. 1996. Bounds on porosity for dielectric logging. Proceedings of European Consortium on Mathematics in Industry, 304–306.

Cole K.S. and Cole R.H. 1941. Dispersion and absorption in dielectrics. *Journal of Chemical Physics* **9**, 341–350.

Freeze A.C. 1966. On the origin of the Sullivan orebody, Kimberly, British Columbia. *Canadian Institute of Mining and Metallurgy*, Special Volume **8**, 263–294.

Garrels R.M., Perry E.A. Jr and Mackenzie F.T. 1973. Genesis of Precambrian iron-formations and the development of atmospheric oxygen. *Economic Geology* **68**, 1173–1179.

Halverson M.O., Zinn W.G., McAlister E.O., Ellis R.B. and Yates W.C. 1981. Assessment of results of broad-band spectral IP field tests. In: *Advances in Induced Polarization and Complex Resistivity*, pp. 295–346. University of Arizona.

Harrington R.F. 1961. *Time-Harmonic Electromagnetic Fields.* McGraw-Hill Book Co.

Hashin Z. and Shtrikman S. 1962. A variational approach to the theory of the effective magnetic permeability of multiphase materials. *Journal of Applied Physics* **33**, 3125–3131.

Lowell J.D. and Guilbert J.M. 1970. Lateral and vertical alteration-mineralization zoning in porphyry ore deposits. *Economic Geology* **65**, 373–408.

McPhedran R.C., McKenzie D.R. and Milton G.W. 1982. Extraction of structural information from measured transport properties of composites. *Applied Physics A* **29**, 19–27.

McPhedran R.C. and Milton G.W. 1990. Inverse transport problems for composite media. *Material Resources Society, Symposium Proceedings* **195**, 257–277.

Milton G.W. 1980. Bounds on the complex dielectric constant of a composite material. *Applied Physics Letters* **37**, 300–302.

Milton G.W. 1981. Bounds on the complex permittivity of a two-component composite material. *Journal of Applied Physics* **52**, 5286–5293.

Pelton W.H. 1977. *Interpretation of induced polarization and resistivity data.* PhD dissertation, University of Utah.

Percival T.J., Bagby W.C. and Radtke A.S. 1988. Physical and chemical features of precious-metal deposits of the western United States (eds R. W. Schafer, J.J. Cooper and P. G. Vikre). Geological Society of Nevada, Symposium Proceedings, pp. 1–34.

Sawkins F.J. and Rye D.M. 1974. Relationship of Homestake-type gold deposits to iron-rich Precambrian sedimentary rocks. *London Institute of Mining and Metallurgy Transactions* **83**, B56–B60.

Wait J.R. 1958. A phenomenological theory of induced electrical polarization. *Canadian Journal of Physics* **36**, 1634–1644.

Wait J.R. 1982. *Geo-electromagnetic.* Academic Press Inc.